IEEE Photonics Journal
An IEEE Photonics Society Publication

Open Access

20 GHz Mode-Locked Laser Diodes With Integrated Optical Feedback Cavities in a Generic Monolithic InP Photonics Platform

Volume 9, Number 5, October 2017

Torrey Thiessen
Joyce K. S. Poon, ***Member, IEEE***

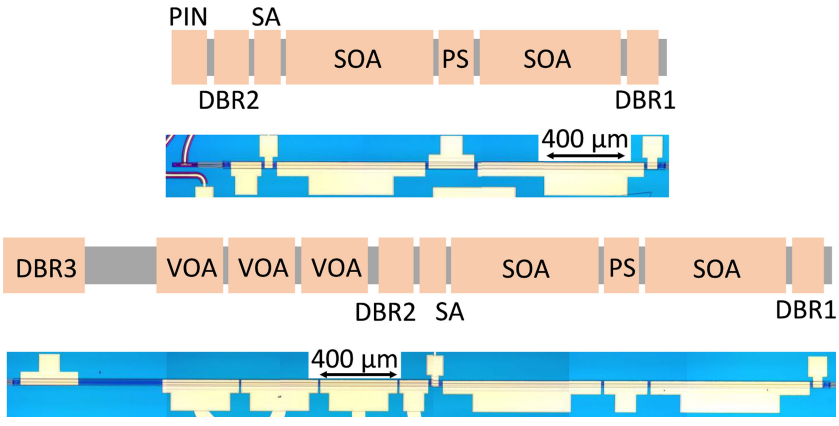

DOI: 10.1109/JPHOT.2017.2731980
1943-0655 © 2017 IEEE

IEEE photonics SOCIETY

IEEE

20 GHz Mode-Locked Laser Diodes With Integrated Optical Feedback Cavities in a Generic Monolithic InP Photonics Platform

Torrey Thiessen and Joyce K. S. Poon, *Member, IEEE*

Department of Electrical and Computer Engineering, University of Toronto, Toronto, Ontario M5S 3G4, Canada

DOI:10.1109/JPHOT.2017.2731980

Manuscript received June 9, 2017; revised July 17, 2017; accepted July 21, 2017. Date of publication July 26, 2017; date of current version August 17, 2017. This work was supported in part by the Natural Sciences and Research Council of Canada and the Canada Research Chairs program and in part by the Seventh Framework programme of the European Union under PARADIGM project 257210.
Corresponding author: Torrey Thiessen (e-mail: torrey.thiessen@mail.utoronto.ca).

Abstract: We investigate integrated mode-locked laser diodes with distributed Bragg reflectors fabricated in the JePPIX-Oclaro indium phosphide photonics platform. The optical and radio-frequency (RF) characteristics of passively mode-locked lasers with and without monolithically integrated feedback cavities were measured and compared. The RF linewidth of the mode-locked laser could be reduced by integrating an optical feedback cavity of a particular length and a tunable magnitude of feedback. A maximum linewidth reduction factor of 1.9 was observed near the onset of mode locking, but increasing the laser optical power tended to lead to unstable operation. Increasing the drive current of the design without feedback also reduced the RF linewidth. A reduction factor of 7.6 was observed.

Index Terms: Diode lasers, laser mode locking, laser feedback, bragg gratings.

1. Introduction

Mode-Locked laser diodes (MLLDs) that produce periodic trains of pulses at high repetition rates in excess of 1 GHz have potential applications as radio-frequency (RF) or mm-wave oscillators [1], [2], in all-optical clock recovery [3], [4], and in data communications [5]. Passively MLLDs (PMLLDs) have the advantage that they do not require an external RF modulation signal. However, the noise properties of passively MLLDs tend to be worse than their hybrid mode-locked counterparts, in which the low frequency phase noise tends to follow that of the RF source [6]–[10]. One technique for reducing RF noise in mode-locked lasers is through optical feedback or photon seeding, wherein a small fraction of the power emitted from the laser is fed back into the laser cavity. This technique has been used to reduce noise in MLLDs through the use of external (off-chip) feedback cavities [7], [11]–[14] and, more recently, with an on-chip feedback cavity in a hybrid silicon platform [15].

Many examples of distributed Bragg reflector (DBR) MLLDs have been demonstrated, utilizing conventional [5], [16]–[21], sampled [22], or chirped gratings [23] as reflectors. When compared to Fabry-Perot (FP) MLLDs, DBR MLLDs offer ease of integration with other components on-chip and

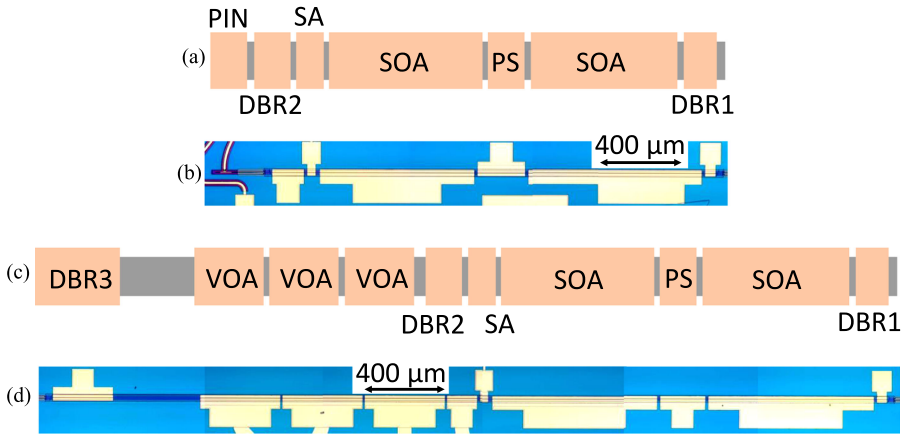

Fig. 1. (a) Schematic of the standalone MLLD with a 20 GHz repetition rate, and (b) the corresponding die photo. (c) Schematic of a MLLD with a 20 GHz repetition rate with a monolithically integrated feedback cavity, and the (d) corresponding die photo.

precise control over central laser wavelength at the cost of narrowed optical bandwidth (limited by the bandwidth of the DBR mirrors) and a corresponding increase in the pulse width.

The noise of mode-locked lasers is described in detail in [24], [25] and an emphasis on the noise of MLLDs is given in [26]. As shown in [27], the RF linewidth, $\Delta\nu_{RF}$, is related to the Schawlow-Townes optical linewidth, $\Delta\nu_{ST}$, by

$$\Delta\nu_{RF} = C_1\Delta\nu_{ST} + C_2 RIN, \tag{1}$$

where RIN is the low frequency relative intensity noise, and C_1 and C_2 are expressions described in [27]. Briefly, C_1 describes the contribution of optical phase noise to RF phase noise and C_2 describes the coupling between variations in pulse energy and timing jitter [15], [27], [28]. The RF linewidth can be reduced through pulse stabilization techniques, such as controlled optical feedback or photon seeding, which can also reduce laser linewidth.

In this work, we used the JePPIX-Oclaro generic monolithic indium phosphide (InP) photonics design kit for the multiproject wafer shuttle run 3 of the PARADIGM program [29], in which the DBR properties and material layers were fixed, to study PMLLDs with a monolithically integrated feedback cavity. Under specific feedback conditions, the RF linewidth could be reduced. Previous analysis of DBR based MLLDs has shown that, like FP MLLDs, the lasers are very sensitive to both the magnitude of the feedback as well as the length of the optical feedback or photon seeding cavity [30]. Improper choice of either may cause the laser to become unstable. In a fully integrated approach, cavity lengths can only be slightly tuned, so we design and compare cavities of various lengths and tune the intensity of the optical feedback.

2. Device Design

Fig. 1 shows the MLLD designs implemented in the JePPIX-Oclaro technology. Fig. 1(a) and (b) are, respectively, the schematic and optical micrograph of the laser without any feedback. Fig. 1(c) and (d) are, respectively, the schematic and optical micrograph of the laser with an integrated feedback cavity. The lasers were designed to operate with a repetition rate around 20 GHz for this proof-of-concept study. The lasers can be designed for other repetition rates by adjusting the cavity lengths. The main laser cavity was nominally identical for the case with and without feedback. The laser cavity was composed of two semiconductor optical amplifiers (SOAs, 830 μm in length), a saturable absorber (SA, 50 μm), and a phase shifter (PS, 225 μm). The SA was formed by reverse biasing a 50 μm long section of SOA, which was the minimum SOA length available on this platform. The phase shifter was based on carrier injection, in order to use a waveguide geometry which was compatible with the rest of the laser design, and allowed for fine tuning of

the repetition rate; however, it was not used in the results to follow. A 10 μm long electrical isolation region was placed between individual active components, including the DBR mirrors, which were tunable through carrier injection. The total length of the laser cavity was 1985 μm, defined as the distance between the start of the two DBR mirrors, which corresponds to a 20 GHz repetition rate assuming a group index of 3.77.

The laser and feedback cavity were terminated by DBR mirrors of varying reflectivities. The grating strength was 50 cm^{-1} for all three DBRs. The expected repetition rate was slightly under 20 GHz due to the penetration depth of the DBR mirrors, which increased the effective cavity length. At the Bragg wavelength, the penetration depth of the DBR mirrors is given by [31]

$$L_{eff} = L \frac{\sqrt{R}}{2\,\mathrm{atanh}(\sqrt{R})}, \tag{2}$$

where R is the reflectance and L is the length of the DBR. The laser cavity was terminated by a low reflectance DBR (DBR1, 50 μm long, designed for R ~6% at the Bragg wavelength, $L_{eff,1}$ ~24 μm) at the front of the cavity for high output power and a moderate reflectance DBR at the rear (DBR2, 150 μm, R ~40%, $L_{eff,2}$ ~64 μm) to allow for coupling between the main cavity and the feedback cavity. Devices without a feedback cavity were terminated by a highly absorbing PIN diode placed after the rear DBR to reduce any residual reflections. A feedback cavity was introduced by placing a high reflectance DBR (DBR3, 300 μm, R ~82%, $L_{eff,3}$ ~90 μm) behind the rear DBR of the laser.

The length of the feedback cavity was chosen such that the pulse being fed back into the laser cavity would arrive just ahead of the main cavity pulse, as is typical in photon seeding experiments. Feedback cavity lengths, defined as the separation between DBR2 and DBR3, of 1585 μm, 1665 μm, 1745 μm, and 1825 μm were implemented for comparison. The lengths between the SA and DBR3 were 1745 μm, 1825 μm, 1905 μm, and 1985 μm, respectively. Thus, a feedback pulse is expected to arrive at the SA 6 ps, 4 ps, 2 ps, or 0 ps in advance of the intracavity pulse, respectively. The penetration depth of the DBR mirrors has negligible effect on the relative pulse timing, as the effective length increase due to the DBR mirrors terminating the main cavity ($L_{eff,1} + L_{eff,2} = 88$ μm) closely matches the penetration depth of a feedback pulse reflecting from DBR3 ($L_{eff,3} = 90$ μm). The magnitude of the feedback was tuned by the three variable optical attenuators (VOAs, 400 μm long) in the feedback cavity. The VOAs were the carrier injection based phase shifters in the design kit. The excess single-pass attenuation in each VOA was 4 dB at a current of 25 mA, and about 5.5 dB for currents greater than 70 mA. Therefore, a maximum attenuation of over 30 dB was possible for the feedback pulse.

3. Experimental Results

3.1. Measurement Setup

To measure the devices, the InP chip was mounted on a stage maintained at 20 °C. Although tunable, the DBRs were left unbiased to avoid introducing excess electrical noise. Multiple fiber-optic splitters were used to allow simultaneous collection of the power, optical spectrum (ANDO AQ6317B), pulse duration (APE pulseCheck USB 50), and RF spectrum (40 GHz Archcom photoreceiver with a 26.5 GHz HP E4407B spectrum analyzer).

3.2. Standalone DBR MLLD

The optical characteristics of the standalone laser (no feedback) are summarized in Fig. 2. The power measurements reported in Fig. 2(a) and (b) refer to the on-chip average power at the spot size converter. Fig. 2(a) shows the L-I characteristics of our laser when various SA bias voltages, V_{SA}, were applied. The threshold gradually increased from 23 mA for $V_{SA} = 0$ V to 34 mA for $V_{SA} = -3$ V. Fig. 2(b) shows the output power as a function of V_{SA} at several values of I_{SOA}. Fig. 2(c) shows the evolution of the optical spectrum when $V_{SA} = -1.5$ V and I_{SOA} was increased from 40 mA to 100 mA. The spectra shows the expected broadening of the spectrum with higher drive current,

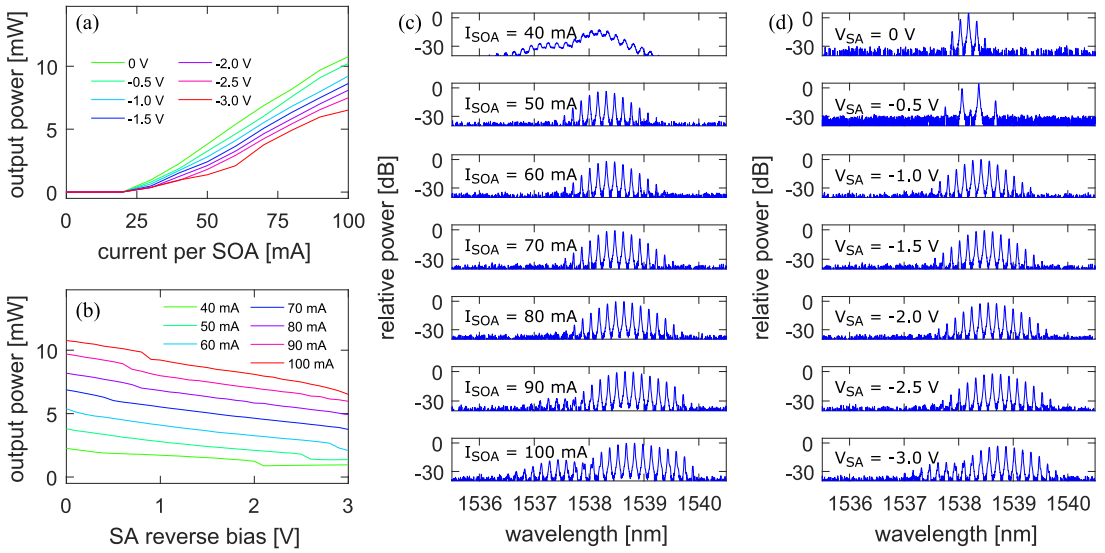

Fig. 2. Optical characteristics of the standalone 20 GHz MLLD without a feedback cavity. The reported optical powers refer to the average power on-chip. (a) L-I curves for the laser as V_{SA} is varied. (b) The output power dependence of the laser on V_{SA} with I_{SOA} ranging from 40 mA to 100 mA. (c) The optical spectrum of the laser with $V_{SA} = -1.5$ V and I_{SOA} ranging from 40 mA to 100 mA. (d) The optical spectrum of the laser with $I_{SOA} = 70$ mA and V_{SA} ranging from 0 V to -3 V.

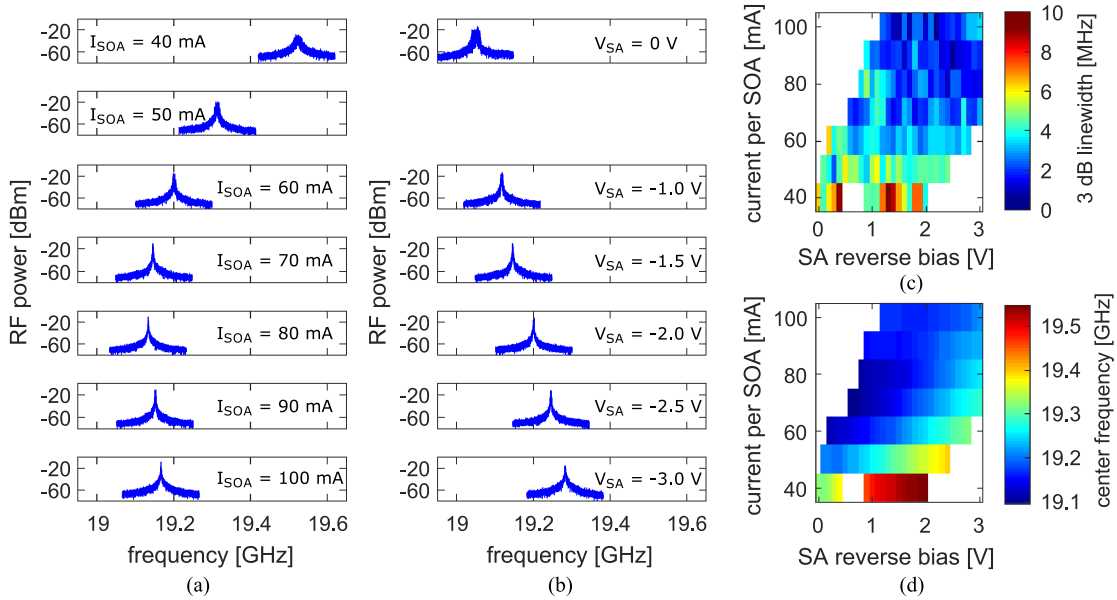

Fig. 3. RF characteristics of the standalone 20 GHz MLLD without a feedback cavity. (a) The RF spectrum of the laser with $V_{SA} = -1.5$ V and I_{SOA} ranging from 40 mA to 100 mA. (b) The RF spectrum of the laser with $I_{SOA} = 70$ mA and V_{SA} ranging from 0 V to -3 V. (c) The RF linewidth as a function of I_{SOA} and V_{SA}. Missing data points indicate the laser did not mode-lock or mode-locked with an RF linewidth greater than 10 MHz. (d) The center frequency of the RF spectrum as a function of I_{SOA} and V_{SA}.

and had a free spectral range of approximately 150 pm, corresponding to about 19 GHz. Fig. 2(d) shows the optical spectrum when $I_{SOA} = 70$ mA and V_{SA} was varied from 0 V to -3 V. The large change in the optical spectrum shown in Fig. 2(d) between -0.5 V and -1 V corresponds to the onset of mode-locking. Stable mode-locking was not observed for $I_{SOA} > 100$ mA.

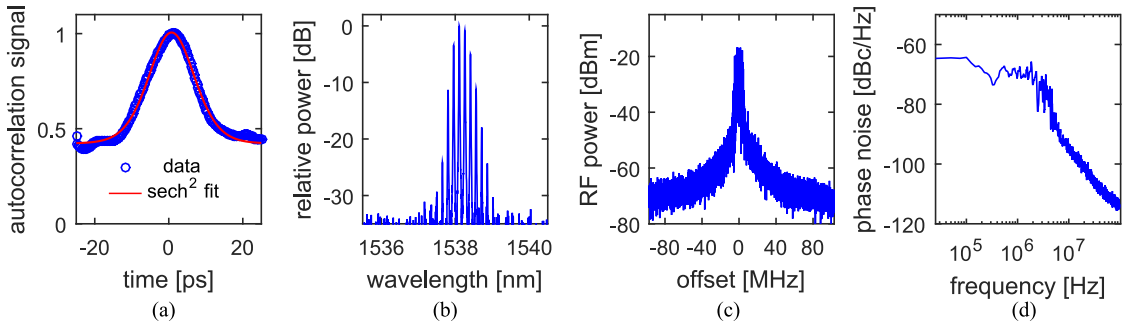

Fig. 4. Characteristics of the standalone 20 GHz MLLD without a feedback cavity. The laser was biased with $I_{SOA} = 50$ mA and $V_{SA} = -0.8$ V. (a) The measured autocorrelation trace in collinear mode and the sech^2 fit shows a 9.4 ps FWHM pulse width. In the collinear mode, the peak-to-background ratio of an ideal autocorrelation trace is 3:1. The measured peak-to-background ratio was 2.38. (b) The optical spectrum shows line spacing corresponding to the repetition rate. (c) The measured RF spectrum is centered at 19.24 GHz. (d) The SSB noise spectrum of the RF signal. The extracted 3 dB RF linewidth was 4.1 MHz.

The RF characteristics of the laser are shown in Fig. 3. Fig. 3(a) and (b) show the evolution of the RF spectrum over the same sets of bias conditions as shown in Fig. 2(c) and (d). The large variation in repetition rate as the bias conditions were changed was due to both the material refractive index changes as well as saturation effects in the SOAs and SA, which would shift the peak position of the pulses and detune the repetition rate from the round-trip frequency of the laser cavity [28]. The missing RF spectrum in Fig. 3(b) corresponds to the optical spectrum in Fig. 2(d), where the optical modes had a free spectral range much greater than 20 GHz. Fig. 3(c) shows the 3 dB linewidth of the RF spectrum over a wide range of bias conditions. The narrowest linewidth, 530 kHz, was obtained with $I_{SOA} = 90$ mA and $V_{SA} = -2.5$ V. Fig. 3(d) shows the center frequency of the RF spectra under the same sets of bias conditions as Fig. 3(c).

The center frequency was slightly under 20 GHz, which is partially due to the penetration depth of the DBR mirrors. Adding the penetration depths, $L_{eff,1}$ and $L_{eff,2}$, to the distance between the DBR mirrors and assuming a group index of 3.77 gives a repetition rate of about 19.2 GHz, in close agreement with the measured values in Fig. 3(d). In Fig. 3 and the results that follow, the center frequencies in the RF spectra exhibited random fluctuations of about ± 1 MHz, which may be due to noise in the experimental setup (e.g., current supplies). Thus, the spectra show "instantaneous" lineshapes on time-scales limited by the acquisition time of the RF spectrum analyzer. The RF spectra have not been averaged.

We next examine in detail in Fig. 4 the optical and RF characteristics for $I_{SOA} = 50$ mA and $V_{SA} = -0.8$ V, which are typical for the laser at the onset of mode-locking. The on-chip power at the spot size converter under these conditions was about 3 mW. Fig. 4(a) shows the autocorrelation trace, performed in collinear mode to maximize the autocorrelation signal. A low pass filter was applied to the interferometric autocorrelation trace to produce the intensity autocorrelation with background shown in Fig. 4(a). The pulse width was obtained by fitting the intensity autocorrelation trace to the autocorrelation of a sech^2 function, and the corresponding full-width at half-maximum (FWHM) pulse width was 9.4 ps. The ideal peak-to-background ratio of the autocorrelation trace is 3:1 [32]. The peak-to-background ratio of the measured autocorrelation trace was 2.38, slightly lower than the ideal. The discrepancy is likely due to pulse-to-pulse timing jitter combined with the pulse averaging, which would would tend to diminish the peak of the autocorrelation signal. Fig. 4(b) shows the optical spectrum when the laser is mode-locked.

Fig. 4(c) and (d) show the RF line centered at 19.24 GHz and the extracted single sideband (SSB) phase noise spectrum. The phase noise spectrum, $L(\nu)$, was extracted from the RF spectrum by the relation

$$L(\nu) = 10 \log_{10} \left(\frac{P_{n,1Hz}(\nu - \nu_0)}{P_{signal}} \right), \tag{3}$$

where $P_{n,1Hz}(\nu - \nu_0)$ is the power at an offset ν from the center frequency, ν_0, normalized to a 1 Hz bandwidth, and P_{signal} is the total power under the curve. The two sides of the phase noise spectrum were averaged (as the RF line is symmetric) and a 5-point running average filter was applied to the data in Fig. 4(d) for display purposes. At large offset frequencies (>5 MHz), the phase noise spectrum rolls off at −20 dB/decade, characteristic of a Lorentzian line shape [33] and a random walk in the phase fluctuations [34]. At lower offset frequencies, the phase noise spectrum shows a sharp roll off, which is characteristic of the transition between the Gaussian and Lorentzian features of a Voigt line shape [33]. The 3 dB linewidth was extracted by fitting a 40 MHz portion of the RF line to a pseudo-Voigt function, as described in [35]. The RF spectrum measurement was taken at a resolution bandwidth and video bandwidth of 100 kHz, and the extracted 3 dB linewidth was 4.1 MHz. The 3 dB linewidth was dominated by the contribution from the Gaussian noise sources, as can be seen in the phase noise spectrum of Fig. 4(d).

3.3. DBR MLLDs With Integrated Feedback Cavities

From the measurements of the devices that each had an optical feedback cavity with a different length, we studied the trends and conditions for the optical feedback that would improve laser performance. The laser cavity was again biased with $I_{SOA} = 50$ mA and $V_{SA} = -0.8$ V, as in the case for the standalone MLLD described in Fig. 4, and the current to the VOAs was varied. The characteristics for the MLLD with the optimal feedback cavity length, 1665 μm, at varying levels of feedback are summarized in Fig. 5. Fig. 5(a) shows the measured autocorrelation traces and sech^2 fits for strong feedback ($I_{VOA} = 0$ mA), near optimal feedback (18 mA) and less than optimal feedback (33 mA). The corresponding FWHM pulse widths were 8.0 ps, 6.2 ps, and 6.3 ps, respectively. The optical spectra in Fig. 5(b) were broader than the case of no feedback in Fig. 4(b) and narrowed as the amount of feedback was reduced. The narrowest RF linewidths were found within a range of 16–32 mA of current per VOA, as is seen in the RF and phase noise spectra of Fig. 5(c) and (d), respectively. Similar optical and RF spectra were found within this range. The FWHM pulse width within this range was about 6.2 ps, which was 34% narrower than the unseeded case [Fig. 4(a)]. The peak-to-background ratio of the autocorrelation function increased to 2.73, indicating that the quality of mode-locking has improved compared to the standalone DBR MLLD. Within this range, the narrowest RF linewidth was 2.1 MHz, a factor of 49% narrower than the standalone case [Fig. 4(c)].

Fig. 6 compares the RF linewidths as a function of VOA current for different lengths of feedback cavity with $I_{SOA} = 50$ mA and $V_{SA} = -0.8$ V. The spread of the data shown in Fig. 6 may be due to phase shifts introduced when tuning the VOAs, which could not be decoupled from attenuation in our measurements. As expected, the linewidths were found to be sensitive to both the feedback cavity length as well as the current applied to the VOAs. A similar relationship between I_{VOA} and linewidth was observed for all feedback cavity lengths, with the lower limit on linewidth determined by the feedback cavity length. As I_{VOA} increased (i.e., the magnitude of the feedback decreased), the linewidths tended to reach a minimum for I_{VOA} between 15 mA and 50 mA before increasing. When I_{VOA} exceeded 50 mA, the performance of the lasers generally degraded, with a rapid decrease in output power, changes in the optical spectra, and broadening of the RF spectra. This degradation may be due to heating of the InP chip. The narrowest linewidths were obtained for a feedback cavity length of 1665 μm. The longest and shortest feedback cavities [Fig. 6(a) and (d)] did not exhibit an improved linewidth over a standalone laser.

4. Discussion

In our devices, we found that optical feedback was an effective technique for reducing RF noise when the laser was operating near the onset of mode-locking. For lasers with a feedback cavity, the narrowest linewidths were obtained when the round-trip distance between the SA and DBR3 was 320 μm shorter than the main cavity round-trip length. Assuming a group index of 3.77

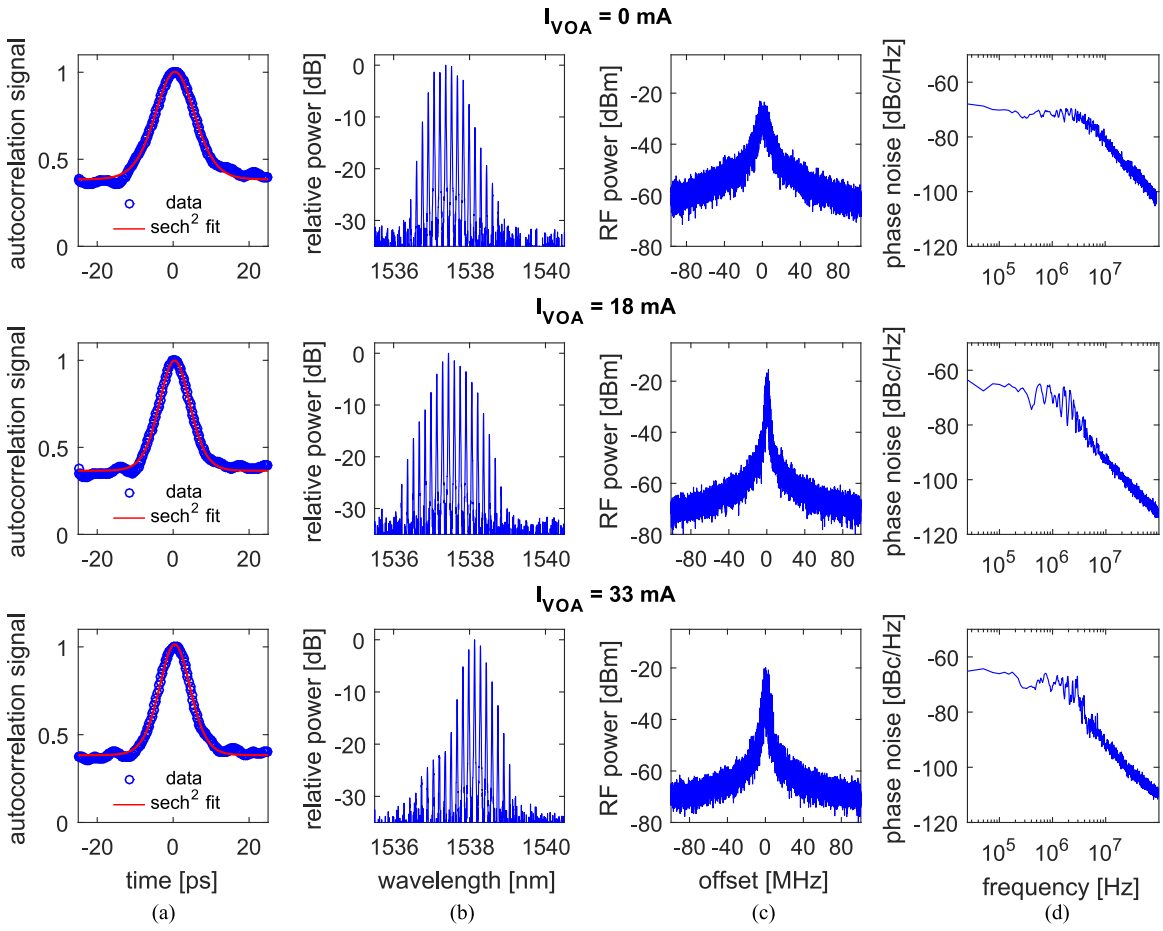

Fig. 5. Characteristics of a 20 GHz MLLD with a feedback cavity and strong feedback ($I_{VOA} = 0$ mA), near optimal feedback ($I_{VOA} = 18$ mA), and less than optimal feedback ($I_{VOA} = 33$ mA). The laser was biased at $I_{SOA} = 50$ mA and $V_{SA} = -0.8$ V, and the length of the feedback cavity was 1665 μm. (a) The measured autocorrelation traces in collinear mode and the sech^2 fit showing FWHM pulse widths of 8.0 ps, 6.2 ps, and 6.3 ps, for $I_{VOA} = 0$ mA, 18 mA, and 33 mA, respectively. (b) The measured optical spectrum is broader compared to Fig. 4(b) and narrows as the feedback is reduced. (c) The RF spectra were centered at 19.45 GHz, 19.57 GHz, and 19.50 GHz, respectively. The narrowest extracted RF linewidth was 2.1 MHz. (d) SSB phase noise spectra extracted from the RF spectra in (c).

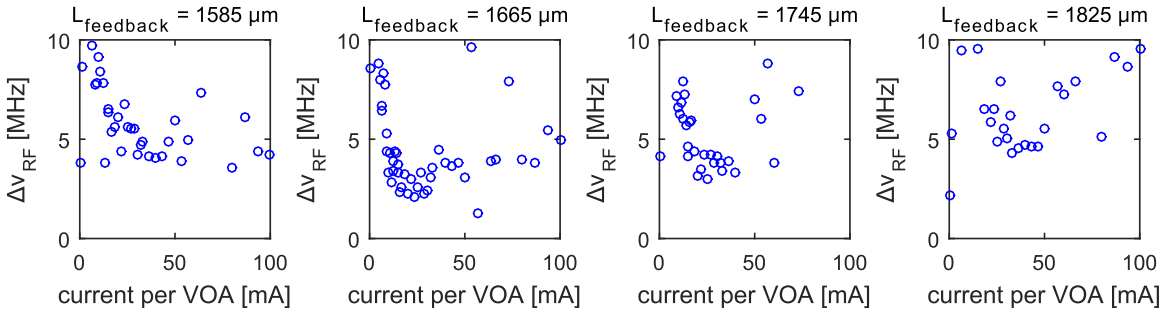

Fig. 6. Comparison of the 3 dB RF linewidths for various feedback cavity lengths, which were obtained by fitting a 40 MHz portion of the RF spectrum with a pseudo-Voigt fit. The laser was biased with $I_{SOA} = 50$ mA and $V_{SA} = -0.8$ V. The sweep of VOA currents was consistent in all measurements. Missing data points indicate that the laser did not mode-lock or mode-locked with a 3 dB linewidth greater than 10 MHz.

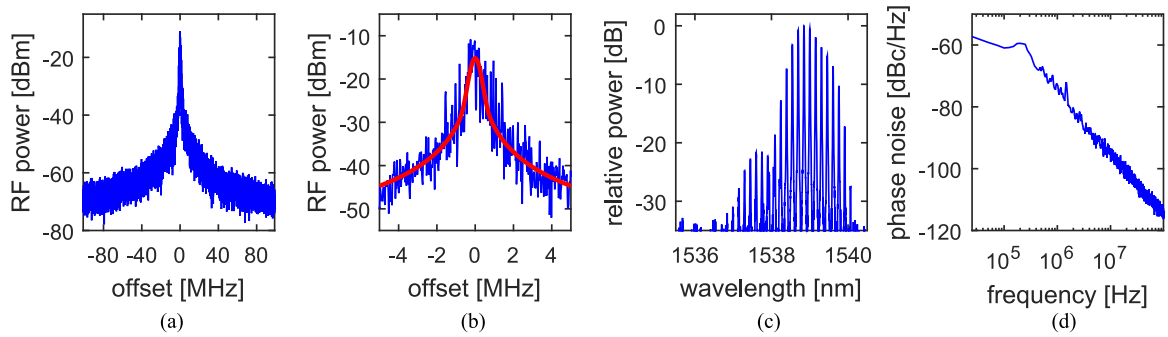

Fig. 7. Characteristics of the 20 GHz MLLD without a feedback cavity when biased at $I_{SOA} = 90$ mA and $V_{SA} = -2.5$ V, which were the optimal bias conditions. (a) RF spectrum centered at 19.21 GHz; (b) raw RF data (blue) and a pseudo-Voigt fit (red); (c) optical spectrum; (d) SSB phase noise spectrum of the RF signal.

(the nominal value), this corresponds to a feedback pulse arriving at the SA about 4 ps in advance of the main cavity pulse.

As the SOA current was increased, the linewidth-narrowing effect from the feedback cavity diminished. Around $I_{SOA} = 70$ mA, the addition of the feedback would often cause the device to become unstable and output pulses at roughly twice the usual repetition rate. The exact cause for this behavior could not be identified.

The RF linewidth narrowing could also be obtained by increasing I_{SOA} in the lasers without a feedback cavity. Fig. 7 shows the detailed characteristics of the laser without a feedback cavity when biased with $I_{SOA} = 90$ mA and $V_{SA} = -2.5$ V. The on-chip power at the spot size converter under these conditions was 6.6 mW. The RF spectrum in Fig. 7(a), which is magnified in Fig. 7(b) and fitted with the pseudo-Voigt function, showed a linewidth of about 530 kHz, which was the narrowest linewidth observed. Fig. 7(c) shows the optical spectrum of the laser output, which was considerably broadened in comparison with Fig. 4(b). The measured pulse width from the autocorrelation trace (not shown) was 9.2 ps. These figures are comparable to other MLLDs fabricated in the JePPIX-Oclaro InP photonics platform [20], [21].

Lastly, passively mode-locked quantum well MLLDs with very low timing jitter and low RF noise use only one quantum well layer to reduce the differential gain and losses [36]. Quantum dot MLLDs are also promising for short pulse and low jitter operation [37]–[39]. The JePPIX-Oclaro InP platform uses multiple quantum wells in the active regions to achieve a high gain. While we were not able to change the number of quantum wells or the layer stack in this generic foundry process, our results suggest that future foundry platforms can consider an alternate layer stack for MLLD applications. In existing foundry platforms, for low noise operation, active or hybrid mode-locking should be pursued.

5. Conclusion

In summary, we have investigated the effects of incorporating a short feedback cavity monolithically to a DBR MLLD realized in the JePPIX-Oclaro generic InP platform. At low bias currents to the SOAs, specific selections of the length and reflection coefficient from the feedback cavity led to a linewidth reduction of 49% compared to the standalone laser without any feedback. At higher SOA currents, feedback caused the laser to become unstable. The narrowest RF linewidth of 530 kHz was achieved with an SOA current of 90 mA and a bias of -2.5 V to the SA without the use of a feedback cavity. The results shown here may be improved by further reducing the optical feedback to the laser to avoid instabilities at higher SOA currents. Increasing the length of the external cavity, which increases its quality factor, would reduce the amount of feedback and may also reduce the linewidth of the optical modes. A phase-only tuning section could also be introduced to the feedback cavity to allow for independent optimization of the feedback magnitude and phase. Lastly, the DBR

mirrors at both ends of the feedback cavity could be replaced with broadband mirrors to simplify the wavelength tuning of the device.

Acknowledgment

The author would like to thank Dr. W. Sacher for his contributions to the chip design and helpful discussions. The chips were fabricated by Oclaro Technology Limited, Caswell, Towcester, United Kingdom. They would also like to thank Dr. M. Wale, Dr. D. Robbins, and Dr. R. Penty for access to the technology.

References

[1] A. Stohr *et al.*, "Millimeter-wave photonic components for broadband wireless systems," *IEEE Trans. Microw. Theory Tech.*, vol. 58, no. 11, pp. 3071–3082, Nov. 2010.
[2] A. R. Criado, C. de Dios, P. Acedo, G. Carpintero, and K. Yvind, "Comparison of monolithic optical frequency comb generators based on passively mode-locked lasers for continuous wave mm-wave and sub-THz generation," *J. Lightw. Technol.*, vol. 30, no. 19, pp. 3133–3141, Oct. 2012.
[3] S. Arahira, "Variable-in, variable-out optical clock recovery with an optically injection-locked and regeneratively actively mode-locked laser diode," *IEEE J. Quantum Electron.*, vol. 47, no. 5, pp. 614–621, May 2011.
[4] S. Arahira, S. Sasaki, K. Tachibana, and Y. Ogawa, "All-optical 160-gb/s clock extraction with a mode-locked laser diode module," *IEEE Photon. Technol. Lett.*, vol. 16, no. 6, pp. 1558–1560, Jun. 2004.
[5] R. Kaiser and B. Huttl, "Monolithic 40-GHz mode-locked MQW DBR lasers for high-speed optical communication systems," *IEEE J. Sel. Topics Quantum Electron.*, vol. 13, no. 1, pp. 125–135, Jan. 2007.
[6] F. R. Ahmad and F. Rana, "Fundamental and subharmonic hybrid mode-locking of a high-power (220 mW) monolithic semiconductor laser," *IEEE Photon. Technol. Lett.*, vol. 20, no. 15, pp. 1308–1310, Aug. 2008.
[7] L. Drzewietzki, S. Breuer, and W. Elsäßer, "Timing jitter reduction of passively mode-locked semiconductor lasers by self- and external-injection: Numerical description and experiments," *Opt. Exp.*, vol. 21, no. 13, pp. 16 142–16 161, Jul. 2013.
[8] C. Ji *et al.*, "Synchronized transform-limited operation of 10-GHz colliding pulse mode-locked laser," *IEEE Photon. Technol. Lett.*, vol. 18, no. 4, pp. 625–627, Feb. 2006.
[9] S. Keyvaninia *et al.*, "Narrow-linewidth short-pulse III-V-on-silicon mode-locked lasers based on a linear and ring cavity geometry," *Opt. Exp.*, vol. 23, no. 3, pp. 3221–3229, Feb. 2015.
[10] G. Carpintero, M. G. Thompson, R. V. Penty, and I. H. White, "Low noise performance of passively mode-locked 10-GHz quantum-dot laser diode," *IEEE Photon. Technol. Lett.*, vol. 21, no. 6, pp. 389–391, Mar. 2009.
[11] L. A. Jiang, K. S. Abedin, M. E. Grein, and E. P. Ippen, "Timing jitter reduction in modelocked semiconductor lasers with photon seeding," *Appl. Phys. Lett.*, vol. 80, no. 10, pp. 1707–1709, Mar. 2002.
[12] C. Y. Lin, F. Grillot, Y. Li, R. Raghunathan, and L. F. Lester, "Microwave characterization and stabilization of timing jitter in a quantum-dot passively mode-locked laser via external optical feedback," *IEEE J. Sel. Topics Quantum Electron.*, vol. 17, no. 5, pp. 1311–1317, Sep. 2011.
[13] G. Fiol, M. Kleinert, D. Arsenijević, and D. Bimberg, "1.3 μm range 40 GHz quantum-dot mode-locked laser under external continuous wave light injection or optical feedback," *Semicond. Sci. Technol.*, vol. 26, no. 1, 2011, Art. no. 014006.
[14] M. Haji *et al.*, "High frequency optoelectronic oscillators based on the optical feedback of semiconductor mode-locked laser diodes," *Opt. Exp.*, vol. 20, no. 3, pp. 3268–3274, Jan. 2012.
[15] S. Srinivasan, E. Norberg, T. Komljenovic, M. Davenport, G. Fish, and J. E. Bowers, "Hybrid silicon colliding-pulse mode-locked lasers with on-chip stabilization," *IEEE J. Sel. Topics Quantum Electron.*, vol. 21, no. 6, pp. 24–29, Nov. 2015.
[16] J. Renaudier, G. H. Duan, J. G. Provost, H. Debregeas-Sillard, and P. Gallion, "Phase correlation between longitudinal modes in semiconductor self-pulsating DBR lasers," *IEEE Photon. Technol. Lett.*, vol. 17, no. 4, pp. 741–743, Apr. 2005.
[17] L. Hou, M. Haji, and J. H. Marsh, "Monolithic mode-locked laser with an integrated optical amplifier for low-noise and high-power operation," *IEEE J. Sel. Topics Quantum Electron.*, vol. 19, no. 4, pp. 1 100 808–1 100 808, Jul. 2013.
[18] R. Kaiser *et al.*, "Tunable monolithic mode-locked lasers on InP with low timing jitter," *IEEE Photon. Technol. Lett.*, vol. 15, no. 5, pp. 634–636, May 2003.
[19] J. Akbar *et al.*, "High-power AlGaInAs mode-locked DBR laser with integrated tapered optical amplifier," *IEEE Photon. Technol. Lett.*, vol. 25, no. 3, pp. 253–256, Feb. 2013.
[20] V. Moskalenko, K. A. Williams, and E. A. J. M. Bente, "Integrated extended-cavity 1.5-μm semiconductor laser switchable between self- and anti-colliding pulse passive mode-locking configuration," *IEEE J. Sel. Topics Quantum Electron.*, vol. 21, no. 6, pp. 40–45, Nov. 2015.
[21] V. Moskalenko, K. A. Williams, and E. A. J. M. Bente, "Pulse narrowing and RF linewidth reduction of integrated passively mode-locked laser in anticolliding design by means of spectral tuning," *IEEE Photon. J.*, vol. 8, no. 4, Aug. 2016, Art. no. 1502810.
[22] L. A. Johansson, Z. Hu, D. J. Blumenthal, L. A. Coldren, Y. A. Akulova, and G. A. Fish,"40-GHz dual-mode-locked widely tunable sampled-grating DBR laser," *IEEE Photon. Technol. Lett.*, vol. 17, no. 2, pp. 285–287, Feb. 2005.
[23] M. J. Strain, P. M. Stolarz, and M. Sorel, "Passively mode-locked lasers with integrated chirped Bragg grating reflectors," *IEEE J. Quantum Electron.*, vol. 47, no. 4, pp. 492–499, Apr. 2011.

[24] R. Paschotta, "Noise of mode-locked lasers (Part II): Timing jitter and other fluctuations," *Appl. Phys. B*, vol. 79, no. 2, pp. 163–173, Jul. 2004.
[25] D. Eliyahu, R. A. Salvatore, and A. Yariv, "Effect of noise on the power spectrum of passively mode-locked lasers," *J. Opt. Soc. Amer. B*, vol. 14, no. 1, pp. 167–174, Jan. 1997.
[26] L. A. Jiang, M. E. Grein, H. A. Haus, and E. P. Ippen, "Noise of mode-locked semiconductor lasers," *IEEE J. Sel. Topics Quantum Electron.*, vol. 7, no. 2, pp. 159–167, Mar. 2001.
[27] F. Kefelian, S. O'Donoghue, M. T. Todaro, J. G. McInerney, and G. Huyet, "RF linewidth in monolithic passively mode-locked semiconductor laser," *IEEE Photon. Technol. Lett.*, vol. 20, no. 16, pp. 1405–1407, Aug. 2008.
[28] S. Arahira and Y. Ogawa, "Repetition-frequency tuning of monolithic passively mode-locked semiconductor lasers with integrated extended cavities," *IEEE J. Quantum Electron.*, vol. 33, no. 2, pp. 255–264, Feb. 1997.
[29] *PARADIGM/EuroPIC Design Manual Version V 5.0 Release Version for PARADIGM Run 3*, JePPIX EuroPIC-PARADIGM, Eindhoven, The Netherlands, 2013.
[30] E. A. Avrutin and B. M. Russell, "Dynamics and spectra of monolithic mode-locked laser diodes under external optical feedback," *IEEE J. Quantum Electron.*, vol. 45, no. 11, pp. 1456–1464, Nov. 2009.
[31] Y. O. Barmenkov, D. Zalvidea, S. Torres-Peiró, J. L. Cruz, and M. V. Andrés, "Effective length of short Fabry-Perot cavity formed by uniform fiber Bragg gratings," *Opt. Exp.*, vol. 14, no. 14, pp. 6394–6399, Jul. 2006.
[32] M. Wollenhaupt, A. Assion, and T. Baumert, *Femtosecond Laser Pulses: Linear Properties, Manipulation, Generation and Measurement*. New York, NY, USA: Springer, 2007, pp. 937–983.
[33] F. Herzel, "An analytical model for the power spectral density of a voltage-controlled oscillator and its analogy to the laser linewidth theory," *IEEE Trans. Circuits Syst. I*, vol. 45, no. 9, pp. 904–908, Sep. 1998.
[34] A. Demir, A. Mehrotra, and J. Roychowdhury, "Phase noise in oscillators: A unifying theory and numerical methods for characterization," *IEEE Trans. Circuits Syst. I*, vol. 47, no. 5, pp. 655–674, May 2000.
[35] P. Thompson, D. E. Cox, and J. B. Hastings, "Rietveld refinement of Debye-Scherrer synchrotron X-ray data from Al_2O_3," *J. Appl. Crystallogr.*, vol. 20, no. 2, pp. 79–83, Apr. 1987.
[36] K. Merghem *et al.*, "Short pulse generation using a passively mode locked single InGaAsP/InP quantum well laser," *Opt. Exp.*, vol. 16, no. 14, pp. 10 675–10 683, Jul. 2008.
[37] M. G. Thompson, A. R. Rae, M. Xia, R. V. Penty, and I. H. White, "InGaAs quantum-dot mode-locked laser diodes," *IEEE J. Sel. Topics Quantum Electron.*, vol. 15, no. 3, pp. 661–672, May 2009.
[38] D. Arsenijević, M. Kleinert, and D. Bimberg, "Breakthroughs in photonics 2013: Passive mode-locking of quantum-dot lasers," *IEEE Photon. J.*, vol. 6, no. 2, pp. 1–6, Apr. 2014.
[39] K. Klaime *et al.*, "23 and 39 GHz low phase noise monosection InAs/InP (113)B quantum dots mode-locked lasers," *Opt. Exp.*, vol. 21, no. 23, pp. 29 000–29 005, Nov. 2013.